Energy Reports 10 (2023) 360–367

Contents lists available at ScienceDirect

Energy Reports

journal homepage: www.elsevier.com/locate/egyr

Research paper

# Inherently boosted switched inductor hybrid converter with AC and DC outputs for DC nanogrid applications

Md Samiullah [a], Mohammed A. Al-Hitmi [b,*], Atif Iqbal [b], Imtiaz Ashraf [a]

[a] Aligarh Muslim University, India
[b] Qatar University, Qatar

ARTICLE INFO

*Article history:*
Received 27 March 2023
Received in revised form 29 May 2023
Accepted 20 June 2023
Available online 4 July 2023

*Keywords:*
Hybrid converter
Nanogrid
High gain
Shoot through
Switched inductor

ABSTRACT

This paper presents a novel hybrid converter which is capable of carrying AC and DC loads simultaneously at different ports. The converter is designed by using a full bridge inverter at the nodes between the active switched inductor based high gain DC-DC converter. After inserting impedance into the current path, the inherent protection against the shoot through that often happens with a voltage source converter (VSI) is established. In addition, the modulation is such that the converter does not have to rely on shoot through to work, like most hybrid converters do. Instead, an extra charging mode has been added. This not only increases the voltage gain but also provides a flexible control with two duty ratios. The steady state operation of the converter is analyzed in five modes and their voltage relations are found out. A suitable pulse width modulation is realized to generate the different modes of operations. A prototype of the proposed converter is developed in the laboratory which is tested for suitable duty ratios operating for a maximum power of 600 W when the input voltage is maintained at 32 V. The converter finds its suitability in the nanogrid/microgrid where different loads are to be supplied from a single source.



## 1. Introduction

The research in the field of nanogrid having renewable energy sources is aimed at improving the design and efficiency of the converters used within the system (Vakacharla et al., 2016a; Bagewadi et al., 2020; Shiluveru et al., 2020; Samal et al., 2021; Husev et al., 2021). It also seeks to enhance power quality for high-quality loads, decrease nanogrid system size, and make its controllability simpler. These goals are accomplished by doing research on various converters especially multi-port converters and their control, switching variations and topological alternatives (Samal et al., 2021; Aman et al., 2019; Subudhi and Krithiga, 2019; Chauhan et al., 2018; Sharma et al., 2016; Prabhala et al., 2014). The AC and DC loads available in these nanogrids can be separately handled by using individual converters connected to the same DC voltage source (solar PV, Battery or Fuel cell - $v_{in}$) as can be seen in the first part of Fig. 1. But the involvement of multiple converters has made the system expensive, and inefficient (Sharmitha et al., 2019; Sreenivasulu et al., 2016; Vakacharla et al., 2016b; Venkatesh et al., 2014). Therefore a hybrid converter with high power density, low losses, and low cost is a good option as this only converter is sufficient to interlink the different class of loads (AC and DC) to the generating station as shown in Fig. 1.

The single output port limits the converter applications to particular type of loads only. The single input multiple output (SIMO) approach for a nanogrid has been carried out in Castle and El Shahat (2017) where a modified boost converter is able to deliver three different levels of DC output voltages. However, this converter is suitable for different loads of similar nature (i.e. only without isolation). To carry the different categories of loads (with and without galvanic isolation), a new design of converter is proposed in Ray and Mishra (2013), where the active switch of the boost converter has been replaced by a four switch H-bridge design and a separate isolated port is taken out. The research carried out in Ray and Mishra (2013) has been put forward by making the converter suitable for AC and DC loads in Ray and Mishra (2014). This hybrid converter was realized by replacing the control switch of a conventional boost converter by a single phase H-bridge inverter such that the shoot through period can be utilized as the duty period of the boost converter. This converter not only provides simultaneous AC and DC outputs but also it can resilient the unwanted shoot through of the conventional VSI and no dead time is required. Much like boost derived hybrid converter in Ray and Mishra (2014), CUK-derived (Sarath and Kanakasabapathy, 2015) and SEPIC derived (Tomy and Thomas, 2017) are proposed that carry AC and DC loads simultaneously and are immune against shoot through. These converters reduce the power conversion stages and increase the power density by

* Corresponding author.
*E-mail address:* m.a.alhitmi@qu.edu.qa (M.A. Al-Hitmi).

https://doi.org/10.1016/j.egyr.2023.06.042

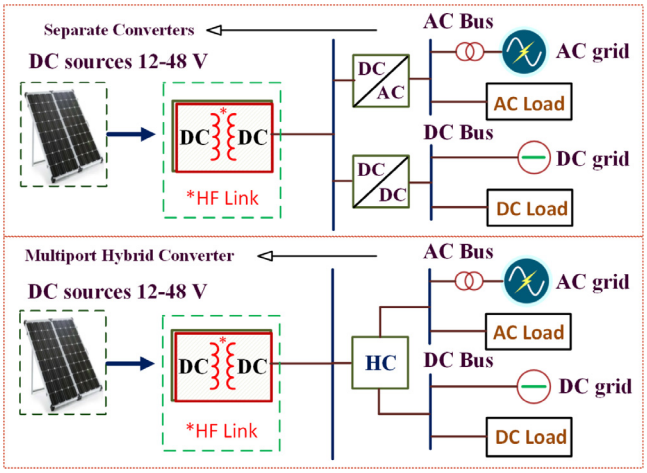


**Fig. 1.** Implementation of a Hybrid Converter with Solar PV in a nanogrid.

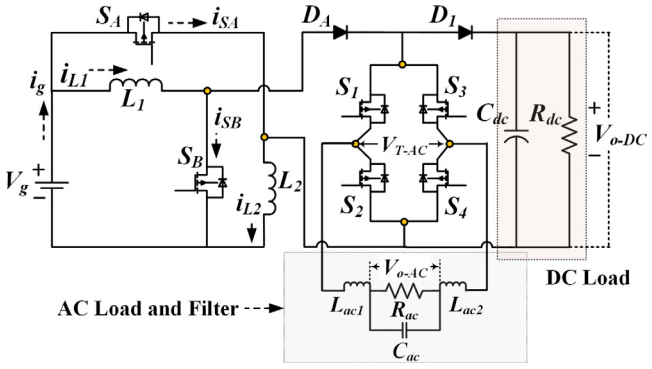


**Fig. 2.** The Proposed Hybrid converter with AC and DC output ports.

providing the compact prototype design. Quadratic Boost derived based converter is introduced in Ahmad et al. (2017) which is capable of providing multiple AC and one DC outputs. This is achieved by replacing the existing primary switch of a quadratic converter by multiple H-bridge circuits connected in either series or in parallel. But this converter becomes complicated in design followed by its intricate control. Moreover, all the hybrid converters in Tang et al. (2021), Ray and Mishra (2014), Dey et al. (2019), Chauhan et al. (2017), Ray and Mishra (2015), Tang et al. (2018) have their entire operation dependent on shoot through period only which restricts their operation to certain low value of duty ratio only. If these converters would be operated for a longer duration of shoot through period, there will be increase in voltage ripples across the switches and the AC voltage will be having more THD owing to the less duration of power modes. Considering the leakage current issues of these Hybrid converters, Highly efficient and reliable inverter concept (HERIC) is utilized in Tang et al. (2019) with improved modulation where the inductor of the boost converter is replaced by two similar inductors placed at the positive and negative rails. In this converter, the number of inductors and switches are increased which intricate the modulation and control. In this paper, a new design of hybrid converter with improved modulation has been introduced which is having the following distinct features.

- Capable of providing AC and DC outputs simultaneously at different ports
- Having provisions of flexible control with the two duty ratios
- High voltage gain compared to the existing hybrid converters owing to the presence of additional charging mode
- Operation of the converter is possible with or without the shoot through
- Compact in size with lesser number of components as of ZSI (Impedance source Inverter) and SBI (switched boost Inverter) based designs

## 2. The proposed hybrid converter

### 2.1. Power circuit

The circuit design of the hybrid converter discussed in this paper is depicted in Fig. 2. The design involves two inductors $L_1$ and $L_2$, which are linked to their respective branch switches $S_1$ and $S_2$, followed by a conventional H-bridge inverter, output diode, AC and DC loads and filters (*LCL* for AC, *C* for DC). The two duty cycles $\delta_{CH}$ and $\delta_{ST}$, in combination with the modulation index $m_A$, are used to regulate the converter. A full steady-state study of the proposed hybrid converter is performed under the premise that the components are ideal and lossless. Moreover, the inductors $L_1$ and $L_2$ are identical and have the same value.

### 2.2. Extended unipolar PWM with charging and ST modes

The proposed hybrid converter has been modulated and controlled by using modified unipolar sine pulse width modulation (SPWM) where two sinusoids ($+v_{sine}$ and $-v_{sine}$) and two dc constant signals ($V_{ST}$ and $--V_{ST}$) are used to generate the required pulses after they are compared with a high frequency triangular carrier wave ($V_{carr}$) as presented in Fig. 3(b). Fig. 3(a) shows the conventional way of generating the controlling pulses and their switching pattern when shoot through insertion is done in ZSI. In the proposed extended modulation where shoot through period is made to remain constant with only two periods and includes a charging duty cycle over the zero mode of inverter which eradicates the dependency of the converter's operation on the shoot through period only. Fig. 4(a) depicts the implementation of simplified logic for the required pattern of signal generation. After using simple mathematics of triangle similarity in Fig. 4(b),

$$\Delta \text{ade} \sim \Delta \text{afg} \Rightarrow \frac{V_{\max}}{T_S/4} = \frac{V_{ST}}{\text{ae}} \tag{1}$$

From Fig. 3, after getting the value of 'ae', the above equation terminates at the following relation,

$$\delta_{ST} = [1 - \frac{V_{ST}}{V_{\max}}]; \ \text{as'ae'} = \frac{\delta_{ST} T_S}{4} \tag{2}$$

The two switches $S_A$ and $S_B$ at the source side controls the charging and discharging of the two inductors which consequently regulates the defined charging mode (CHM). The time period for which direct charging through these switches happen is $\delta_{CH} T_S$. This mode (CHM) can be varied by varying the difference ($V_x$− offset voltage) between $V_{ST}$ and $v_{sine}$. However it is quite evident that the charging interval faces a difference in frequency owing to the dependency on sinusoidal modulation signal $v_{sine}$. Therefore a variable frequency unipolar PWM has been employed which regulates the charging period by varying the voltage $V_x$. A mathematical relation can be derived between $V_x$ and $\delta_{CH}$. From Fig. 4(b), let us consider the following relations;

$$v_{carr}(t_2) = v_{\text{sine}}(t_2); \tag{3}$$

$$V_x = v_{\text{sine}}(t_1) - v_{\text{sine}}(t_2) \Rightarrow v_{carr}(t_1) = v_{\text{sine}}(t_2) + V_x \tag{4}$$

$$\text{and, } t_2 - t_1 = \frac{\delta_{CH} T_S}{2} \tag{5}$$

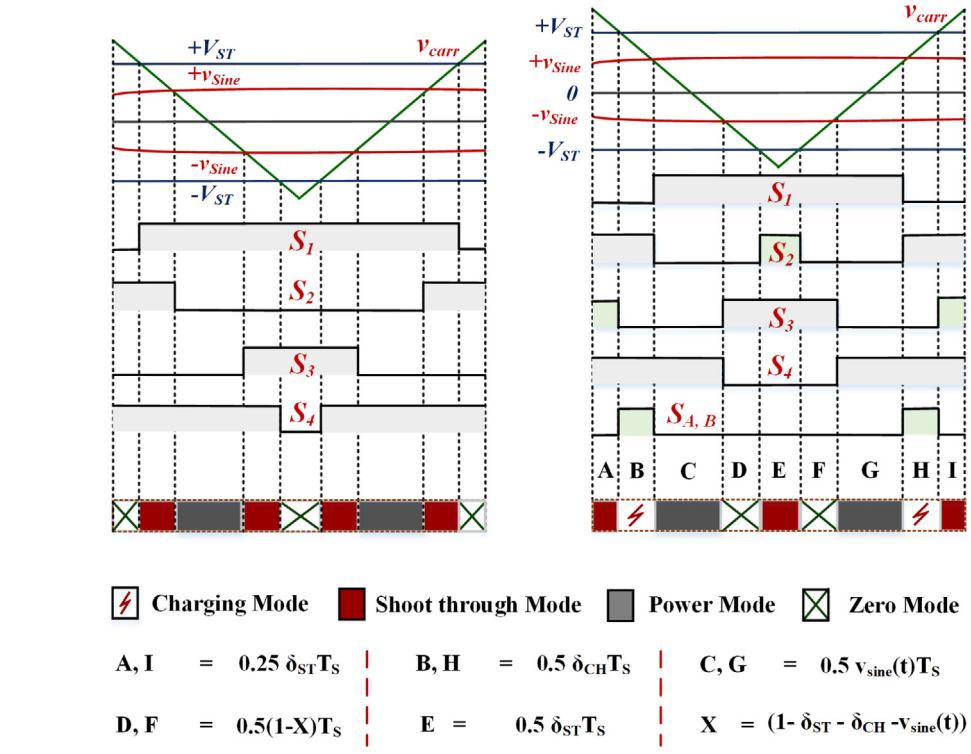


**Fig. 3.** Modulation strategies and generation of different modes of operation (a) Without charging mode (b) with insertion of charging mode.

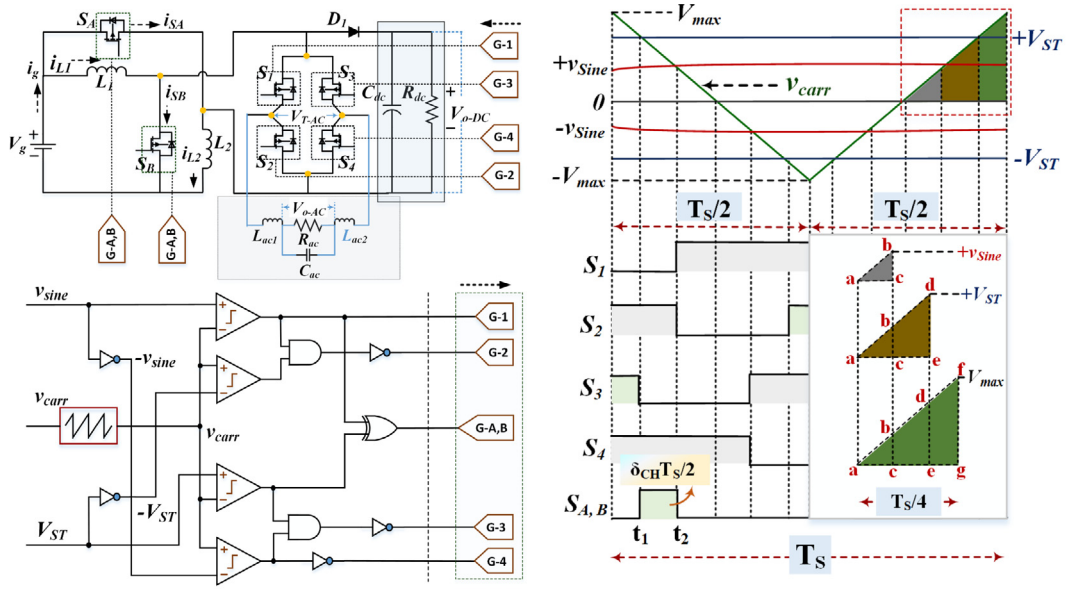


(a) Modulation realization by logic gates

(b) Analysis of duty realtions with the modulating signals

**Fig. 4.** Modulation strategies and their analysis.

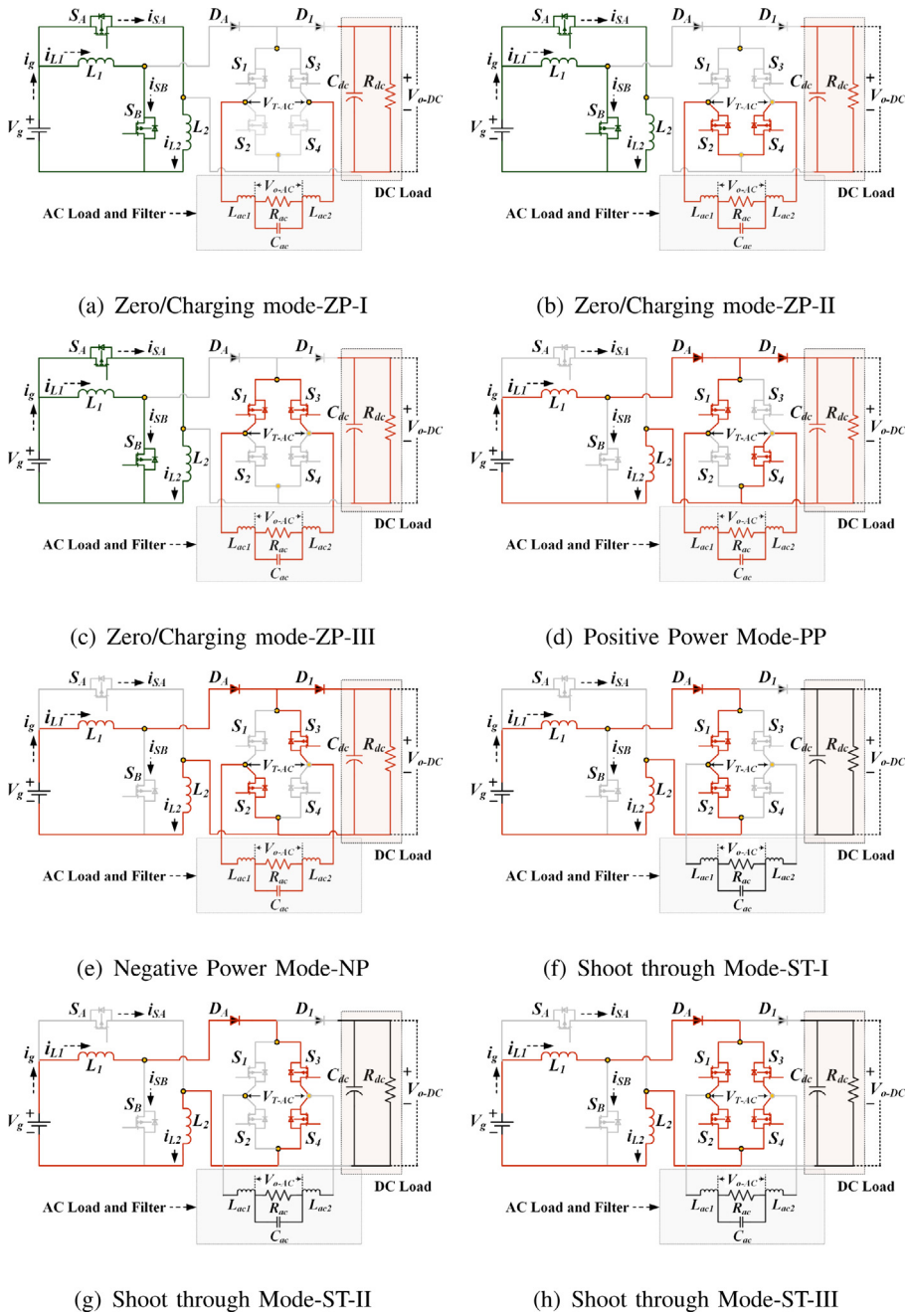


(a) Zero/Charging mode-ZP-I (b) Zero/Charging mode-ZP-II

(c) Zero/Charging mode-ZP-III (d) Positive Power Mode-PP

(e) Negative Power Mode-NP (f) Shoot through Mode-ST-I

(g) Shoot through Mode-ST-II (h) Shoot through Mode-ST-III

**Fig. 5.** Circuit configurations on various possible modes of operation.

From Fig. 4(b), the equation for the triangular carrier wave can be written as;

$$v_{carr}(t) = \frac{-V_{\max}}{(T_S/4)}(t - \{T_S/4\}) \tag{6}$$

Therefore;

$$t_1 = \frac{T_S}{4}(1 - \frac{v_{\sin e}(t_1) + V_x}{V_{\max}}),\ t_2 = \frac{T_S}{4}(1 - \frac{v_{\sin e}(t_2)}{V_{\max}}) \tag{7}$$

After solving above equations, the following relation is obtained;

$$\delta_{CH} = [\frac{V_{ST} - v_{\sin e}}{2V_{\max}}] \tag{8}$$

## 3. Converter operation and design

### 3.1. Operating modes during steady state condition

The converter modes of operation are shown in Fig. 5. The various modes are represented by different equivalent circuit structures. As shown in Fig. 3, the functioning of the proposed hybrid converter may be brought out from various alternative combinations to a specified logic. The detailed explanation of the modes of operation are presented below:

#### 3.1.1. Mode I: [Charging mode]

This mode of the proposed converter depicts the charging (CHM) mode when all the two inductors are directly charged from

the DC supply at the input by turning ON the switches $S_A$ and $S_B$. The time period for this mode is assumed to be $\delta_{CH}T_S$. The following equations define the converter's behavior during this mode:

$$\begin{cases} V^{I}_{L1} = V^{I}_{L2} = V_S, V^{I}_{Co} = V_o \\ I^{I}_{S} = I^{I}_{L1} + I^{I}_{L2} \end{cases} \tag{9}$$

*3.1.2. Mode II: [Positive power mode]*

This mode corresponds to the positive power (PPM) mode of the inverter when the switches $S_1$ and $S_3$ are turned ON keeping all other switches turned OFF. The voltage that appears across the AC load is equal to $+Vo$ (DC) and the same voltage is maintained across the DC load. The inductors are discharging in series through the loads. The circuit current path and the equivalent models are shown in Figs. 3(b) and 4(b) respectively. This voltages and currents in this mode are given as follows:

$$\begin{cases} V^{II}_{L1} = V^{II}_{L2} = \dfrac{V_S - v_{AC}}{2}; v_{AC} = V_O; V^{II}_{C1} = V_o \\ I^{III}_{L1} = I^{III}_{L2} = I^{III}_{S} \end{cases} \tag{10}$$

*3.1.3. Mode III: [Shoot through mode]*

The avoidable mode of conventional VSI has intentionally been introduced here, called the Shoot through mode. This condition is realized either after turning ON the switches of the same leg ($S_1-S_2$, $S_3-S_4$) or after switching all the switches ($S_1-S_2$, $S_3-S_4$) ON at the same time. The three possible alternatives (STM-I, STM-II and STM-III) are presented in table I. This mode is usually avoided in conventional VSI as it may lead to very high inrush current owing to the short circuiting of the supply. However, in the proposed converter this mode is intentionally provided as it offers a current path for the inductors to be magnetized again and therefore we get another time period of charging denoted by $\delta_{ST}T_S$. The voltage and current equations are:

$$\begin{cases} V^{II}_{L1} = V^{II}_{L2} = \dfrac{V_S}{2}; V^{II}_{C1} = V_o \\ I^{II}_{L1} = I^{II}_{L2} = I^{II}_{S} \end{cases} \tag{11}$$

*3.1.4. Mode IV: [Negative power mode]*

This mode corresponds to the negative power (NPM) mode of the inverter when the switches $S_2$ and $S_4$ are turned ON keeping all other switches turned OFF. The voltage that appears across the AC load is equal to $-V_o$ (DC) and a constant voltage $V_o$ is maintained across the DC load. The inductors are discharging in series through the loads. The circuit current path and the equivalent models are shown in Figs. 3(b) and 4(e) respectively. This voltages and currents in this mode are given as follows:

$$\begin{cases} V^{II}_{L1} = V^{II}_{L2} = \dfrac{V_S - v_{AC}}{2}; v_{AC} = -V_O; V^{II}_{C1} = V_o \\ I^{III}_{L1} = I^{III}_{L2} = I^{III}_{S} \end{cases} \tag{12}$$

*3.1.5. Mode V: [Zero power mode]*

This particular mode (ZPM) bear a resemblance to the zero mode of a conventional H bridge inverter when either of the three possible conditions exists from table I. As previously mentioned, the switching combinations S1-S3, S2-S4 essentially reflect the zero mode. Utilization of this mode otherwise, does not affect the voltage output of a converter. Part of this mode has been utilized for charging of the inductances as discussed earlier. The time remaining after all of the previously described modes is the overall duration for this mode.

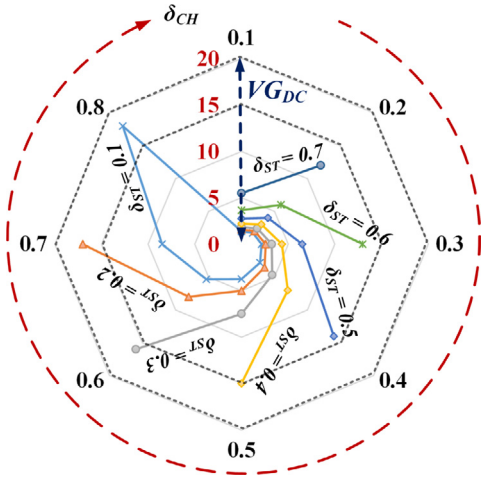


**Fig. 6.** DC voltage gain *Vs* the two duty ratios.

*3.2. Steady state voltage gain and power equations*

Using voltage second balance on inductor $L_1$ and small approximation, the DC voltage gain can be obtained by:

$$\underbrace{\int_0^{\delta_{CH}T_S} V^{I}_{L1}dt}_{P} + \underbrace{\int_0^{\delta_{ST}T_S} V^{II}_{L1}dt}_{Q} + \underbrace{\int_0^{(1-k)T_S} V^{III}_{L1}dt}_{R} = 0 \tag{13}$$

where $k = (\delta_{CH} + \delta_{ST})$. After solving (8), the DC voltage boosting factor is obtained as:

$$G_{CCM}(DC) = \frac{V_o(DC)}{V_{in}} = \frac{1 + \delta_{CH}}{1 - \delta_{CH} - \delta_{ST}} \tag{14}$$

The AC voltage obtained at the other port of the load side is supplied from the boosted DC which later is governed with the modulation index ($m_{AC}$) of the controlling signal. Inspired by the conventional VSI, the AC voltage gain can be obtained as:

$$G_{AC} = \frac{V_o(AC - Peak)}{V_{in}} = \frac{m_{AC}(1 + \delta_{CH})}{(1 - \delta_{CH} - \delta_{ST})} \tag{15}$$

The modulation index ($m_{AC}$) has a well-defined range from 0 to 1. The DC output is the function of $\delta_{ST}$ and $\delta_{CH}$ whereas AC depends on modulation index and the DC output. Although, this converter is capable of being controlled independently with the different duty cycles with boosted outputs with minimum duty period of shoot through mode, the following equality relation still upholds:

$$m_{AC} + \delta_{ST} + \delta_{CH} \leq 1 \tag{16}$$

The peak AC voltage can be obtained from the following relation as obtained in the Eq. (17):

$$V_o(AC - Peak) = \frac{m_{AC}(1 + \delta_{CH})}{(1 - \delta_{CH} - \delta_{ST})} V_{in} \tag{17}$$

The DC voltage gain corresponding to the different combinations of the two duty ratios are plotted in Fig. 6. To ensure the suitable AC and DC voltage outputs, the DC output must always be greater than the peak AC grid/load voltage. The same analysis can be followed up to get the power equations of the converter. The DC power is coming up to be:

$$P_{o-(DC)} = \frac{(1 + \delta_{CH})^2}{R_{O-DC}(1 - \delta_{CH} - \delta_{ST})^2} V_{in}^2 \tag{18}$$

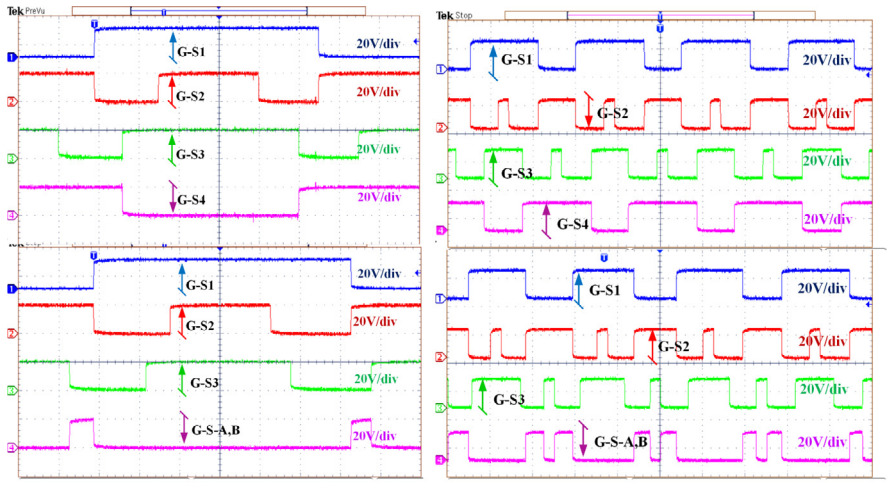


(a) Pulses for a single cycle (b) Pulses for multiple cycles

**Fig. 7.** Generation of switching pulses for experimentation.

Similarly, the instantaneous AC power can be calculated as:

$$p_o(AC) = \frac{(v_{o-AC})^2}{R_{o-AC}} = \frac{(v_{o-Peak})^2}{2R_{o-AC}} - \frac{(v_{o-Peak})^2}{2R_{o-AC}} \cos(2\omega t) \tag{19}$$

The AC power equation as mentioned above has two components, the first one denotes the steady state real power consumed by the load and another indicates the time varying instantaneous AC power.

### 3.3. Design analysis of the components

The passive filters used in the circuit has to be analyzed perfectly in order to mitigate the ripples at different ports of the converter. In the case of grid connection of the DC port, not a significant amount of voltage spike is expected. Therefore the conventional design approach based on the allowable ripples can be used for $C_o$ which is given as:

$$C_o \geq P_{o-(DC)} \times \frac{[\ \delta_{CH} + \delta_{ST}\ ]}{[\ V_{out}(DC) \times \Delta V_{Co} \times f\ ]} \tag{20}$$

Similar to the above, the inductor $L_1$ at the input side of the converter is given as:

$$L_1 \geq V_{in} \times [\delta_{CH} + \delta_{ST}/2] \times [\Delta i_{L1} \times f\ ]^{-1} \tag{21}$$

The filter at the AC grid/load side is mandatory and there is a variety of available choices. The most commonly used filters are *L*, *LC* and *LCL* type. Using a single *L* filter at the AC port not only increases the size but also lacks the standard. The *LC* filter too upholds major issues while being used in the grid-connected inverter. Therefore, *LCL* filter is comparatively a better choice which has slightly smaller size and reduced costs. The design of this filter has a well-known elaborated literature available for the conventional grid connected VSI. While designing the values of inductors, the significantly higher value than the critically required values are chosen to ensure the expected operation of the converter.

## 4. Experimental results

The proposed hybrid converter and its control is finally justified by developing and experimenting on an MOSFET based hardware prototype. The controlling signals to the switches were generated from a TI microcontroller TMS320F28379 development kit followed by driver boards. The experimental testing were carried out with a certain primary goals and objectives in consideration. The initial motivation was to generate and validate the control signals for the proposed converter such that the converter can perform the way it was analyzed theoretically. The second target was to confirm simultaneous AC and DC operation at elevated voltage levels. The subsequent goal was to lower the shoot through duty ratio $\delta_{ST}$ while maintaining a high voltage at the output terminals. This objective also validates the converter's versatility in controlling a certain voltage level without being fully reliant on a single shoot through duty ratio unlike many reported converters. Fig. 7 shows the gate pulses when $v_m > 0$ for different switches of the converter. As mentioned in Section 2, the charging period duty cycle $\delta_{CH}$ was generated using a variable frequency unipolar PWM. For DC output control, this mode supplements the shoot through mode and extends the controllability of the converter. Fig. 8(b) shows the steady state voltages and currents at AC and DC output ports of the converter. The achieved AC peak voltage for a 32 V input voltage is 30.5 V (corresponding rms value is 21.2 V/50 Hz for a modulation index of 0.3), with a significantly boosted voltage of 103 V at the DC port of the converter even when the duty ratios are very nominal i.e. $\delta_{ST} = 0.5$ and $\delta_{CH} = 0.19$. The DC load and AC load are selected as 200 and 30 Ω respectively serving the prototype with 470 and 85 Watts respectively. In Fig. 8(d), AC voltage, current along with the line to line terminal AC voltage without filter have been depicted. Moreover, the inductor current (avg- $i_L = 2.4$ A) within the acceptable range of variation has also be shown on the same plot and can be observed its continuity with the basic charging–discharging behavior. Fig. 8(c) depicts a more detailed zoomed-in view of Fig. 8(b) for a single switching cycle. The other important parameters such as voltage across the switches $S_{A,B}$ and diode $D_o$ are depicted in Fig. 8(e). It can be observed that different levels of voltage are available across the switches and diode as predicted earlier in the theoretical analysis. Moreover the converter is also tested with inductive load and the wave plots of the voltages and current in that case has been shown in Fig. 8(f). A variation in the voltage and current phases can be easily observed there.

## 5. Comparative analysis

This section compares the performance of the proposed hybrid converter to that of existing converters in the literature. In compared to the basic topology (cascade or parallel connection

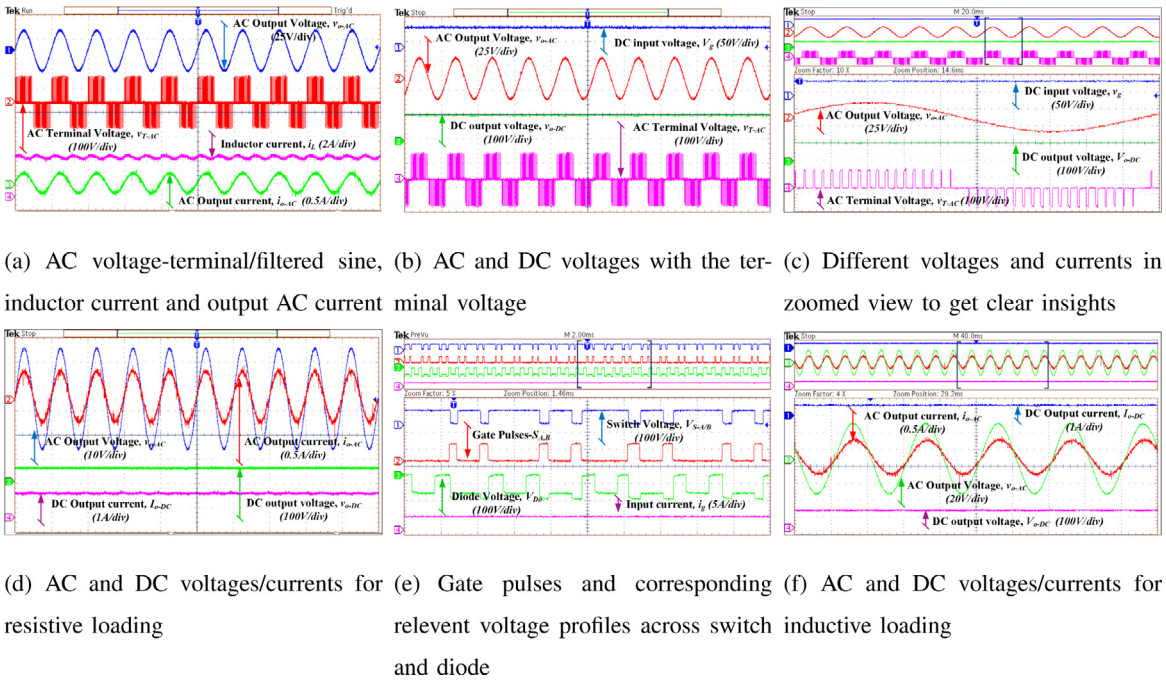


(a) AC voltage-terminal/filtered sine, inductor current and output AC current

(b) AC and DC voltages with the terminal voltage

(c) Different voltages and currents in zoomed view to get clear insights

(d) AC and DC voltages/currents for resistive loading

(e) Gate pulses and corresponding relevent voltage profiles across switch and diode

(f) AC and DC voltages/currents for inductive loading

**Fig. 8.** Important Experimental results.

of VSI and a DC/DC Converter) of a hybrid structure, the presented converter avoids dead time settlement and do not need a compensation circuit by providing a shoot through operating mode similar to that of a ZSI or switched boost inverter. Moreover the additional advantage of using this particular architecture is summarized below:

### *5.1. Simultaneous AC and DC operation with inherent immunity against EMI and noise*

The proposed hybrid converter allows simultaneous operation of AC and DC loads with a single DC source at the input. Unlike conventional VSI, this impedance network based hybrid converter allows inherent protection against excessively high current when shoot through occurs because of noise or EMI. During shoot through, the inductances at the input limit the current through the switches and ensures a stable operation similar to ZSI (Peng, 2003) or SBI (Ravindranath et al., 2012).

### *5.2. Boosted DC and AC operation at lower duty cycles*

It is a well-known concept that in the linear modulation range, a standard traditional VSI cannot deliver a voltage greater than the input DC supply. But the hybrid converter introduced here is able to establish a higher voltage at the dc link followed by a significantly higher rms voltage at the AC terminal. It is also a general advice to not operate the boost converter at higher duty ratios as it will lead to unwanted peaks and diode recovery issues because of very less discharging time of the inductors used in the circuit. This issue has also been tackled easily by utilizing the switched inductor at the input side of the converter which is being charged in parallel and discharge in series to feed the load and allows the converter to operate at lower duty ratios.

### *5.3. Operation with or without shoot through*

Most of the traditional approach of Hybrid converter do not show potency against shoot through and thus need extra circuit and control. On the other hand the recent converters as mentioned in the introduction do have their complete dependency on the shoot through mode only as it is providing the charging line to the passive components. However a better approach should be the converter with independent outputs while resilient of the shoot trough if it stuck to the system. It is therefore an unavoidable dependency of these converters. However, the proposed converter operation rely on two different duty cycles $\delta_{ST}$ and $\delta_{CH}$ generated simply by providing an additional charging mode without interfering the power modes of the converter. This flexibility therefore allows it to operate with or without shoot through duty cycle.

### *5.4. Lower number of passive components and higher power density*

The other configurations of hybrid converter usually have higher number of passive components compared to the proposed switched inductor hybrid converter. A comparison of different related converters is made in the table III. Even the ZSI which is capable of providing only AC does have two inductors and two capacitors whose consistent delicate design is always a problem. Moreover hybrid converter such as SBI also possesses comparatively more number of elements.

### *5.5. Flexibility in control options*

As mentioned earlier the proposed switched inductor based hybrid converter is being controlled with two duty cycles $\delta_{ST}$ and $\delta_{CH}$. Therefore the voltage relation is a function of these two variables leading to many possible combination of values for a particular output. Voltage control at the DC link and hence to the output ports can be attained by three possible ways- $\delta_{ST}$ can be fixed while $\delta_{CH}$ can be altered, $\delta_{CH}$ can be fixed while $\delta_{ST}$ can be changed, and both $\delta_{ST}$ and $\delta_{ST}$ can be altered to attain the required voltage.

## 6. Conclusion

In this paper, a novel design of a hybrid converter is discussed. This converter has been developed to connect multiple loads of different nature i.e. AC and DC to a single DC source. In addition to having multiple ports, the proposed converter has high voltage gain owing to its switched inductor based design. The converter is also immune to shoot through such that shoot through period is intentionally provided along with the charging period. AC and DC loads of 200 Ω and 30 Ω are used to test and validate the performance. The switching frequency is kept at 10 kHz, and the AC line frequency is 50 Hz. At a duty ratio of 0.5 and 0.2 (respectively for $\delta_{ST}$ and $\delta_{CH}$), the converter can deliver 103 V at the DC port and 30.5 V (Peak) at the AC port for an input voltage of 32 V DC with a modulation index of 0.3. An *LCL* filter is designed and used to keep the AC voltage under the recommended THD range. With the designed prototype of 600 W, the obtained AC and DC powers are 470 W and 85 W respectively with an efficiency of 92.5%.

## CRediT authorship contribution statement

**Md Samiullah:** Conceptualization, Software and hardware validation, Writing – original draft. **Mohammed A. Al-Hitmi:** Supervision, Review and editing. **Atif Iqbal:** Supervision, Work validation, Review and editing. **Imtiaz Ashraf:** Supervision and review.

## Declaration of competing interest

This is to confirm that the authors do not have any conflict of interest.

## Data availability

No data was used for the research described in the article.

## Acknowledgments

This publication was made possible by Qatar University Research grant# [QUCP-CENG-2022-571] from the Qatar University, Qatar. The statements made herein are solely the responsibility of the authors. he APC for the article is funded by the Qatar National Library, Doha, Qatar.

## References

Ahmad, A., Bussa, V.K., Singh, R.K., Mahanty, R., 2017. Quadratic boost derived hybrid multi-output converter. IET Power Electron. 10 (15), 2042–2054. http://dx.doi.org/10.1049/iet-pel.2017.0171.

Aman, A., Bussa, V.K., Singh, R.K., 2019. A Minimum Phase Dual Output Hybrid Converter for Off-Grid Applications. In: 2019 IEEE Industry Applications Society Annual Meeting, IAS 2019. IEEE, pp. 1–6. http://dx.doi.org/10.1109/IAS.2019.8912386.

Bagewadi, M.D., Chobe, C.R., Jagtap, P.S., Siddiquee, M., Dambhare, S.S., 2020. Buck-boost derived interleaved hybrid converter for residential nanogrid applications. IET Power Electron. 13 (2), 377–388. http://dx.doi.org/10.1049/iet-pel.2019.0521.

Castle, O.D., El Shahat, A., 2017. Single-input-multi-output (simo) converter for nano-grids applications. In: SoutheastCon 2017. IEEE, pp. 1–5.

Chauhan, A.K., Kumar, R.R., Raghuram, M., Singh, S.K., 2017. Extended Buck-Boost derived hybrid converter. In: 2017 IEEE Industry Applications Society Annual Meeting, IAS 2017, 2017-January. pp. 1–8. http://dx.doi.org/10.1109/IAS.2017.8101766.

Chauhan, A.K., Raghuram, M., Kumar, R.R., Singh, S.K., 2018. Effects and Mitigation of Nonzero DCM in Buck-Boost-Derived Hybrid Converter. IEEE J. Emerg. Sel. Top. Power Electron. 6 (3), 1470–1482. http://dx.doi.org/10.1109/JESTPE.2017.2771331.

Dey, S., Bussa, V.K., Singh, R.K., 2019. Transformerless Hybrid Converter with AC and DC Outputs and Reduced Leakage Current. IEEE J. Emerg. Sel. Top. Power Electron. 7 (2), 1329–1341. http://dx.doi.org/10.1109/JESTPE.2018.2883243.

Husev, O., Matiushkin, O., Vinnikov, D., Roncero-Clemente, C., Kouro, S., 2021. Novel Concept of Solar Converter with Universal Applicability for DC and AC Microgrids. IEEE Trans. Ind. Electron. 0046 (c), http://dx.doi.org/10.1109/TIE.2021.3086436.

Peng, F.Z., 2003. Z-source inverter. IEEE Trans. Ind. Appl. 39 (2), 504–510.

Prabhala, V.A., Gouribhatla, V.S.P., Sat, M., Fajri, P., Ferdowsi, M., 2014. A multiport DC-DC converter with high voltage gain. In: 2014 IEEE 36th International Telecommunications Energy Conference (INTELEC). null, pp. 1–8. http://dx.doi.org/10.1109/INTLEC.2014.6972228, URL https://www.semanticscholar.org/paper/5cbc29cfa580547ee5bb13d9794ede5cc43a7a30.

Ravindranath, A., Mishra, S.K., Joshi, A., 2012. Analysis and PWM control of switched boost inverter. IEEE Trans. Ind. Electron. 60 (12), 5593–5602.

Ray, O., Mishra, S., 2013. A multi-port converter topology with simultaneous isolated and non-isolated outputs. In: IECON 2013-39th Annual Conference of the IEEE Industrial Electronics Society. IEEE, pp. 7118–7123.

Ray, O., Mishra, S., 2014. Boost-derived hybrid converter with simultaneous DC and AC outputs. IEEE Trans. Ind. Appl. 50 (2), 1082–1093. http://dx.doi.org/10.1109/TIA.2013.2271874.

Ray, O., Mishra, S., 2015. Integrated hybrid output converter as power router for renewable-based nanogrids. In: IECON 2015 - 41st Annual Conference of the IEEE Industrial Electronics Society. pp. 1645–1650. http://dx.doi.org/10.1109/IECON.2015.7392337.

Samal, S.K., Bussa, V.K., Singh, R.K., Mahanty, R., 2021. Wide Operating Range Minimum Phase Interleaved Hybrid Converter with Reduced Leakage Current. IEEE Trans. Ind. Appl. 57 (2), 1545–1558. http://dx.doi.org/10.1109/TIA.2020.3045953.

Sarath, R., Kanakasabapathy, P., 2015. Switched-capacitor/switched-inductor ćuk-derived hybrid converter for nanogrid applications. In: 2015 International Conference on Computation of Power, Energy, Information and Communication. ICCPEIC, IEEE, pp. 0430–0435.

Sharma, A., Pramod, B., Singh, R.K., Mahanty, R., 2016. Interleaved hybrid boost converter with simultaneous DC and AC outputs for micro-source applications. In: ECCE 2016 - IEEE Energy Conversion Congress and Exposition, Proceedings. (i), http://dx.doi.org/10.1109/ECCE.2016.7855212.

Sharmitha, D., Lalitha, S., Jeevitha, B., 2019. A novel converter topology for nanogrid application. URL https://www.semanticscholar.org/paper/d8683484847e7e9f3092aab69a9d8ec57c5f84bf.

Shiluveru, K., Singh, A., Ahmad, A., Singh, R.K., 2020. Hybrid Buck-Boost Multioutput Quasi-Z-Source Converter with Dual DC and Single AC Outputs. IEEE Trans. Power Electron. 35 (7), 7246–7260. http://dx.doi.org/10.1109/TPEL.2019.2960268.

Sreenivasulu, T., Ravindra, K., Ravikumar, T., 2016. Analysis of switched boost inverter based on DC nanogrid application. URL https://www.semanticscholar.org/paper/1ae0d923084a617618d72f81eafeb2c10c1d89ec.

Subudhi, P.S., Krithiga, S., 2019. Topological Study of Derived Converters- A review. In: Proceedings of the 2019 2nd International Conference on Power and Embedded Drive Control, ICPEDC 2019. IEEE, pp. 225–230. http://dx.doi.org/10.1109/ICPEDC47771.2019.9036711.

Tang, Z., Su, M., Sun, Y., Cheng, B., Yang, Y., Blaabjerg, F., Wang, L., 2019. Hybrid UP-PWM Scheme for HERIC Inverter to Improve Power Quality and Efficiency. IEEE Trans. Power Electron. 34 (5), 4292–4303. http://dx.doi.org/10.1109/TPEL.2018.2858784.

Tang, Z., Su, M., Sun, Y., Wang, H., Guo, B., Yang, Y., 2018. Hybrid UP-PWM for single-phase transformerless photovoltaic inverter to improve zero-crossing distortion. In: Proceedings - 2018 IEEE International Conference on Industrial Electronics for Sustainable Energy Systems, IESES 2018, 2018-January. pp. 370–375. http://dx.doi.org/10.1109/IESES.2018.8349904.

Tang, Z., Yang, Y., Wan, J., Blaabjerg, F., 2021. Hybrid transformerless PV converters with low leakage currents: Analysis and configuration. IET Renew. Power Gener. http://dx.doi.org/10.1049/rpg2.12029.

Tomy, A., Thomas, A.J., 2017. Sepic derived hybrid converter with simultaneous AC and DC outputs. In: 2016 IEEE Annual India Conference, INDICON 2016. http://dx.doi.org/10.1109/INDICON.2016.7838883.

Vakacharla, V.R., Raghuram, M., Singh, S.K., 2016a. Hybrid Switched Inductor Impedance Source Converter - A Decoupled Approach. IEEE Trans. Power Electron. 31 (11), 7509–7521. http://dx.doi.org/10.1109/TPEL.2016.2535783.

Vakacharla, V.R., Raghuram, M., Singh, S., 2016b. Hybrid switched inductor impedance source converter—A decoupled approach. IEEE Trans. Power Electron. 31, 7509–7521. http://dx.doi.org/10.1109/TPEL.2016.2535783, URL https://www.semanticscholar.org/paper/d2b04be3bbd01d5ffc2f7c55bfdd4bb2830c4630.

Venkatesh, S., Vathsal, S., Prasad, S., 2014. Switched boost inverter for standalone DC nanogrid applications. URL https://www.semanticscholar.org/paper/b2dd699dc27cfb0b9f7b674c88d3ef85998bcf42.